Journal of Thermal Stresses

ISSN: (Print) (Online) Journal homepage: https://www.tandfonline.com/loi/uths20

Temperature-dependent models for wave velocity of oil sand

Hui Qi, Jing Ba & José M. Carcione

To cite this article: Hui Qi, Jing Ba & José M. Carcione (11 Oct 2023): Temperature-dependent models for wave velocity of oil sand, Journal of Thermal Stresses, DOI: 10.1080/01495739.2023.2256806

To link to this article: https://doi.org/10.1080/01495739.2023.2256806

JOURNAL OF THERMAL STRESSES
https://doi.org/10.1080/01495739.2023.2256806

Taylor & Francis
Taylor & Francis Group

Temperature-dependent models for wave velocity of oil sand

Hui Qi[a], Jing Ba[b], and José M. Carcione[b,c]

[a]College of Geosciences and Engineering, North China University of Water Resources and Electric Power, Zhengzhou, China; [b]School of Earth Sciences and Engineering, Hohai University, Nanjing, China; [c]National Institute of Oceanography and Applied Geophysics – OGS, Trieste, Italy

ABSTRACT

Knowledge of how temperature affects the oil–sand acoustic response is useful to exploit these reservoir rocks with seismic methods. We propose three models: double-porosity coherent potential approximation (CPA), lower-bound Hashin–Shtrikmann (HS^-), and contact cement (CC), based on different spatial distributions of heavy oil and temperature and frequency-dependent empirical equations. The shear modulus and S-wave velocity are affected by temperature in all the cases. Moreover, the properties of oil sands with heavy oil as a continuous matrix and higher viscosity are more sensitive to temperature. The models can provide theoretical support for the establishment of rock physical models in heavy oil reservoirs so as to quantitatively characterize the seismic response changes caused by thermal mining.

ARTICLE HISTORY
Received 1 May 2023
Accepted 13 August 2023

KEYWORDS
Heavy oil; oil sand; rock-physics models; spatial distribution; temperature; wave response

1. Introduction

Unconventional hydrocarbon resources are gradually becoming the focus of petroleum exploration and production. Particularly, heavy oil sand is a specific type of resource with huge reserves and understanding the acoustic properties is useful to improve its seismic detection. The high viscosity of heavy oil leads to different properties compared to those of conventional sandstone reservoirs, and specific models are required to describe the wave response.

Heavy oil behaves as a solid at low temperatures, but melts with increasing temperature, thus, decreasing the shear modulus of the sand [1]. The laboratory measurements can provide reliable data for a better quantitative interpretation of the elastic properties of heavy oil-saturated rocks [2–6]. To understand these properties on the basis of measured data, appropriate rock physical models are required [7–13]. Wolf et al. [14] used a Maxwell viscoelastic model [15] to describe the wave attenuation of bitumen-saturated sands. Ciz and Shapiro [16] proposed an extended Gassmann (EG) model [17], and estimated the temperature dependence of the elastic moduli. This model reduces to the classical Gassmann equation [18], for a pore fluid. Kato and Han [19] established an empirical model based on ultrasonic velocity measurements and Gassmann equation. Gurevich et al. [8] adopted the coherent potential approximation method (CPA) to analyze the effects of fluid viscosity and temperature on elastic waves in saturated rocks. Heavy oil can be considered as a viscoelastic medium. Das and Batzle [20] combined the self-consistent approximation [21] with the differential effective medium theory [22–24]. Qi et al. [25] developed a double-porosity CPA model, which considers a temperature-dependent oil viscosity and a microscopic pore structure.

CONTACT Jing Ba jba@hhu.edu.cn School of Earth Sciences and Engineering, Hohai University, Nanjing, China.

Heavy oil behaves as a solid when the temperature is below the liquid point, and the rock elastic properties are mainly affected by the distribution of the oil [9]. This distribution can be divided into three types [7, 9]. At high temperatures heavy oil is a fluid and the distribution has no effect [9]. However, at low temperatures, there is an effect on the elastic properties. Leurer and Dvorkin [26] used the Hertz–Mindlin grain contact model [27] and viscoelasticity. Batzle et al. [28, 29] showed that heavy oil may cement the sand grains [9, 30]. Guo and Han [7] proposed three types infill distributions.

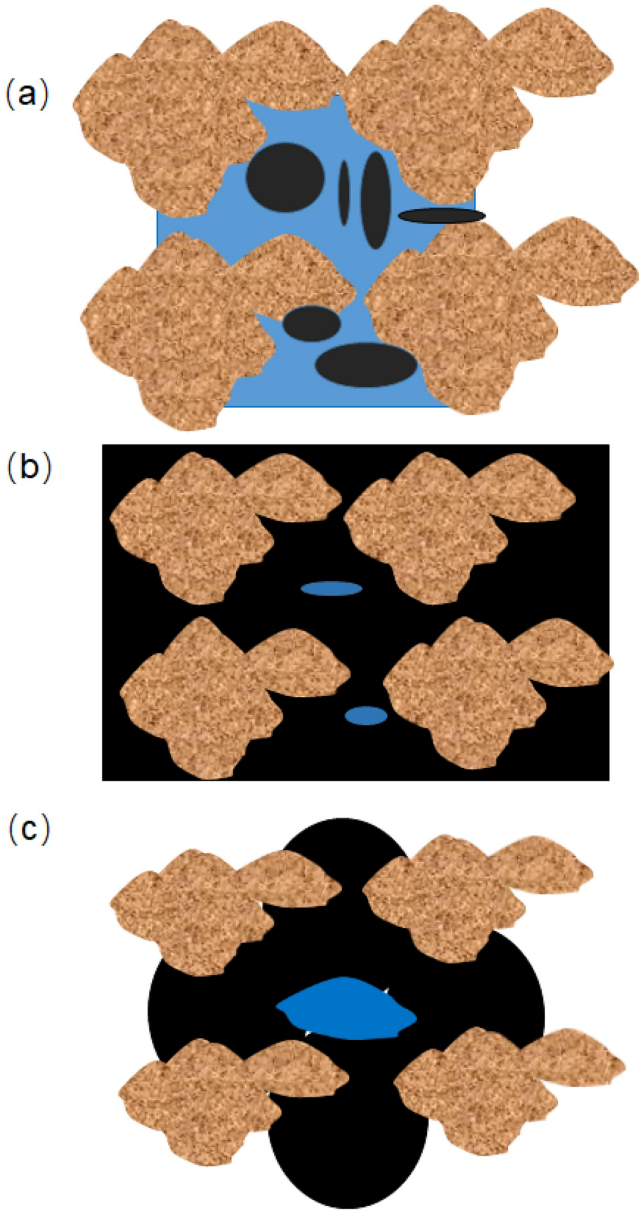

Figure 1. Distributions of heavy oil in sands (a) as a pore infill; (b) as a continuous matrix; (c) cementing the sand grains. The brown, black, and blue colors represent grains, heavy oil, and water, respectively.

Here, we consider the CPA, Hashin–Shtrikman lower bound (HS$^-$), and contact cement model (CC) [21, 30, 31] to analyze the effects of oil distribution on the temperature-dependent physical properties, where this distribution is estimated from ultrasonic data.

2. Theoretical models

2.1. Model I

In this case, heavy oil is the pore infill (see Figure 1a), but conventional models based on the Gassmann and Biot equations cannot be used [8, 18, 32, 33]. Heavy oil exhibits Newtonian fluid properties at high temperatures and behaves as a quasi-solid at room temperature. We adopt a temperature-dependent double-porosity CPA model [25]. When the fluid concentration is low, the solid-fluid mixture is treated as a solid with a specific shape of fluid the inclusions. When the solid content is low, we assume a suspension of grains in a high-viscosity fluid [8, 12, 21]. The equations are

$$\phi_1(K_f - K)P^{f1} + \phi_2(K_f - K)P^{f2} + (1-\phi)(K_s - K)P^s = 0, \tag{1}$$

$$\phi_1(G_f - G)Q^{f1} + \phi_2(G_f - G)Q^{f2} + (1-\phi)(G_s - G)Q^s = 0, \tag{2}$$

where K and G are the bulk and shear moduli of the rock, respectively, sub-indices "s" and "f" refer to the grains and pore infill, P and Q are shape factors [21, 34], ϕ_1 is the stiff porosity, ϕ_2 is the crack/soft porosity, and $\phi = \phi_1 + \phi_2$ is the total porosity. The crack porosity is obtained with the method proposed by David and Zimmerman [35],

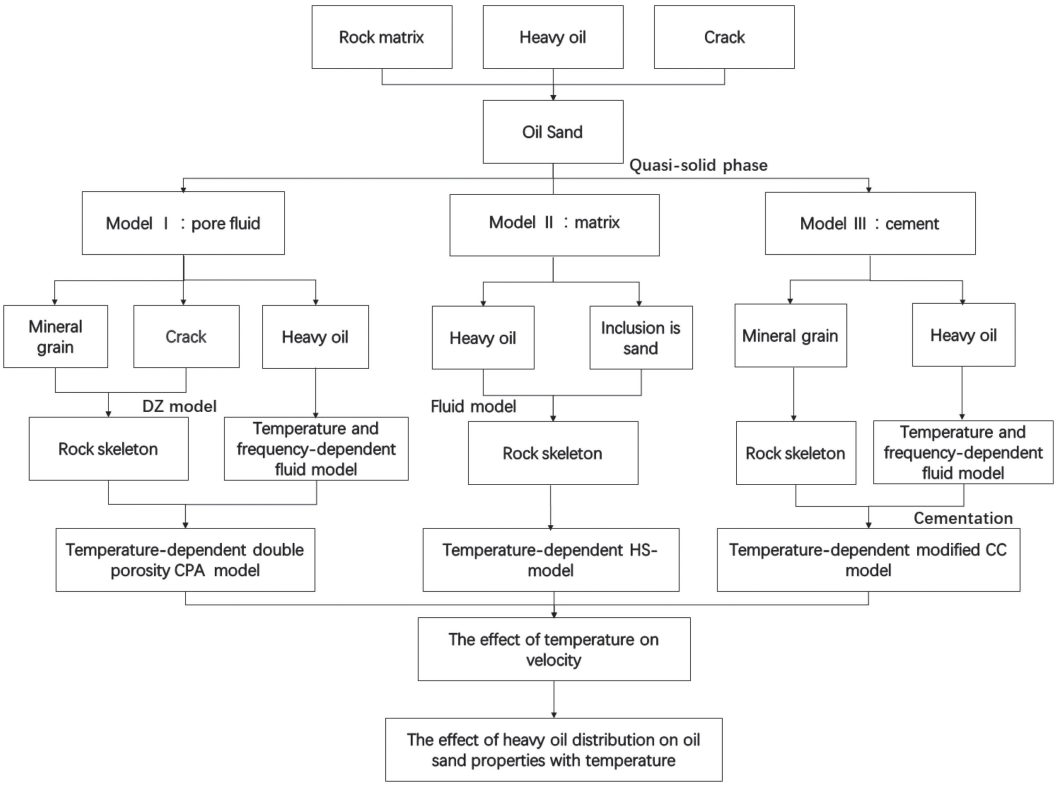

Figure 2. Workflow of the temperature-dependent models of oil sands.

$$\phi_2(T,p) = \frac{4\pi\alpha_p\beta}{3}, \tag{3}$$

where β is crack density, p is effective pressure, and α_p is the crack aspect ratio.

The Maxwell model [14, 36, 37] describes the infill shear modulus,

$$G_f(T) = \frac{i\omega\tau G_\infty}{i\omega\tau + 1}, \tag{4}$$

where G_∞ is the modulus at high frequencies, ω is the angular frequency, $i = \sqrt{-1}$, and $\tau = \eta(T)/G_\infty$ is a relaxation time, with $\eta(T)$ the viscosity as a function of temperature.

Equations (3) and (4) are substituted into Eqs. (1) and (2), and the effective bulk modulus $K_{n+1}(T)$ and shear modulus $G_{n+1}(T)$ of Model I can be obtained by iterations. The result is

$$K_{n+1}(T) = \frac{\phi_1 K_f P_n^{f1} + \phi_2 K_f P_n^{f2} + (1-\phi) K_s P_n^s}{\phi_1 P_n^{f1} + \phi_2 P_n^{f2} + (1-\phi) P_n^s}, \tag{5}$$

$$G_{n+1}(T) = \frac{\phi_1 G_f Q_n^{f1} + \phi_2 G_f Q_n^{f2} + (1-\phi) G_s Q_n^s}{\phi_1 Q_n^{f1} + \phi_2 Q_n^{f2} + (1-\phi) Q_n^s}. \tag{6}$$

The iterative process requires the initial K_1 and G_1, which can be computed by using the Voigt–Reuss–Hill (V–R–H) average [38–41].

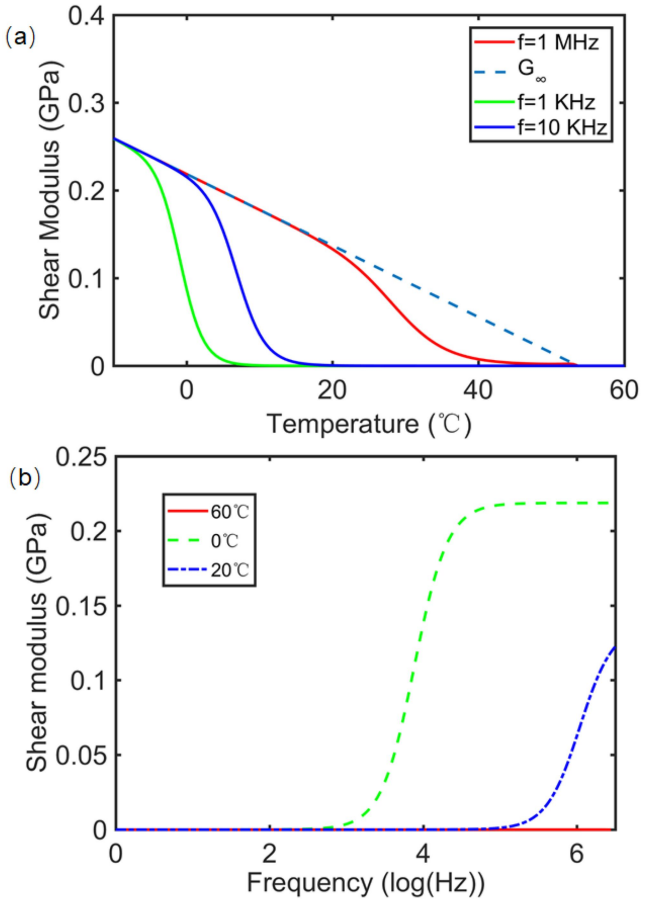

Figure 3. Shear modulus of heavy oil (API = 6.6°) as a function of temperature (a) and frequency (b).

Then, the P- and S- wave velocities are

$$V_{\mathrm{P}(n+1)} = \sqrt{\frac{K_{n+1}(T) + 4G_{n+1}(T)/3}{\rho}}, \tag{7}$$

$$V_{\mathrm{S}(n+1)} = \sqrt{\frac{G_{n+1}(T)}{\rho}}, \tag{8}$$

where ρ is the bulk density.

2.2. Model II

In this case, we have a continuous soft matrix and the sand grains are inclusions (see Figure 1b). When inclusions are harder than the matrix, moderate deviations from sphericity do not have a large effect on the factors of P and Q [42]. If several components of the rock are very different from each other (e.g., minerals and pore fluids), the upper and lower bounds are quite separate. The HS^{-}equations can well describe the moduli in the case of suspended grains in the pore fluid [43]. Thus, the HS^{-} equations apply [9, 31, 44]

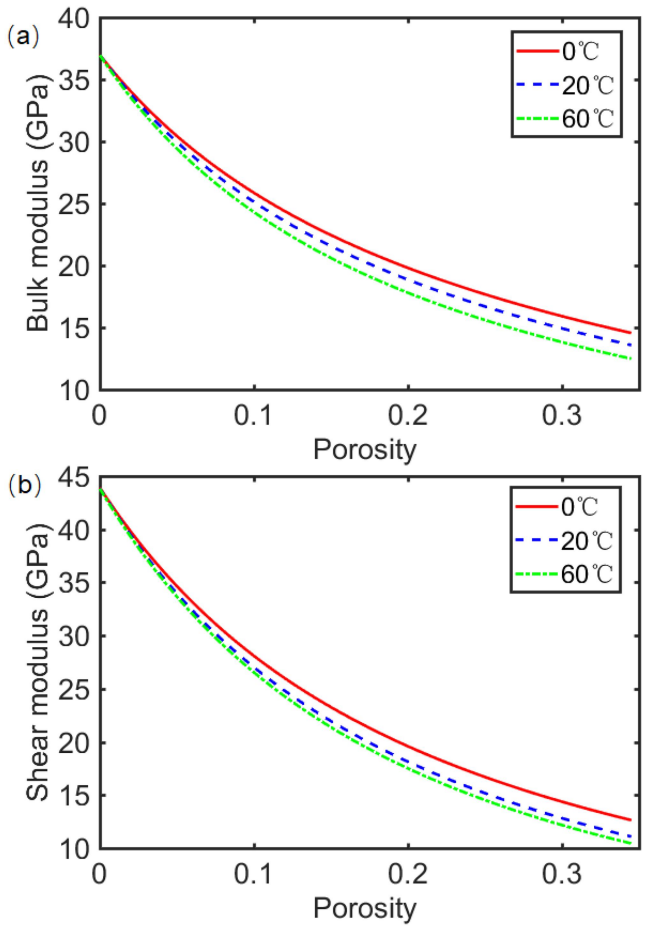

Figure 4. Bulk (a) and shear (b) moduli of Model I as a function of porosity.

$$K(T) = K_f(T) + \frac{(1-\phi)}{\left(K_s - K_f(T)\right)^{-1} + \phi\left(K_f(T) + 4G_f(T)/3\right)}, \tag{9}$$

$$G(T) = G_f(T) + \frac{(1-\phi)}{\frac{1}{\left(G_s - G_f(T)\right)} + \frac{2\phi\left(K_f(T)+2G_f(T)\right)}{5G_f(T)\left(K_f(T)+4G_f(T)/3\right)}}. \tag{10}$$

Substituting Eq. (4) into Eqs. (9) and (10), we obtain the effective moduli. If the pores contain water, these moduli are taken as the solid moduli of Eqs. (1) and (2). Then, the effective moduli can be obtained by iterations.

2.3. Model III

Heavy oil acts as cement at grain contacts (see Figure 1c). Guo and Han [7] obtained the effective moduli with a modified CC model proposed by Han et al. [45, 46]. Incorporating the effects of temperature and frequency, an extended CC model is derived as [30, 45, 46],

$$K = \frac{G_f(T)(1-\nu_f)}{1-2\nu_f}\frac{m(1-\phi_0)}{3(1+e)}S_n, \tag{11}$$

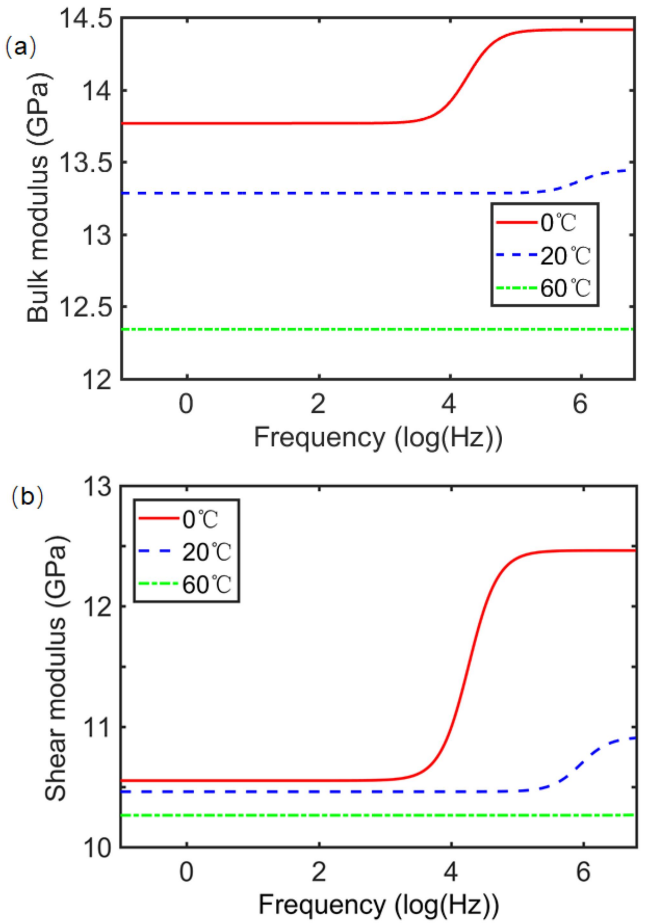

Figure 5. Bulk (a) and shear (b) moduli of Model I as a function of frequency.

$$G=\frac{3}{5}K+\frac{3G_f(T)m(1-\phi_0)}{20(1+e)}S_\tau, \tag{12}$$

where m is the coordination number, ϕ_0 is the critical porosity, e is the contact thickness, which is the ratio of the minimal half distance between two adjacent grains to the radius of the grains, v_f is Poisson's ratio of heavy oil, and $G_f(T)$ is the shear modulus of heavy oil, dependent of temperature and frequency as shown in Eq. (4), S_n and S_τ are normal and tangential contact stiffnesses, respectively, which depend on the total amount of cement, contact thickness, and properties of the heavy oil cementation. The total amount of cement is quantitatively described by the cementation radius r [45, 46],

$$r=\left(-2e+2\sqrt{e^2+\frac{4(\phi_0-\phi)}{3m(1-\phi_0)}}\right)^{-\frac{1}{2}}, \tag{13}$$

$$r=\left(\frac{2(\phi_0-\phi)}{3(1-\phi_0)}\right)^{-\frac{1}{2}}. \tag{14}$$

Equation (13) describes the distribution of heavy-oil cement at grain contacts, and Eq. (14) corresponds to a uniform distribution on the grain surface.

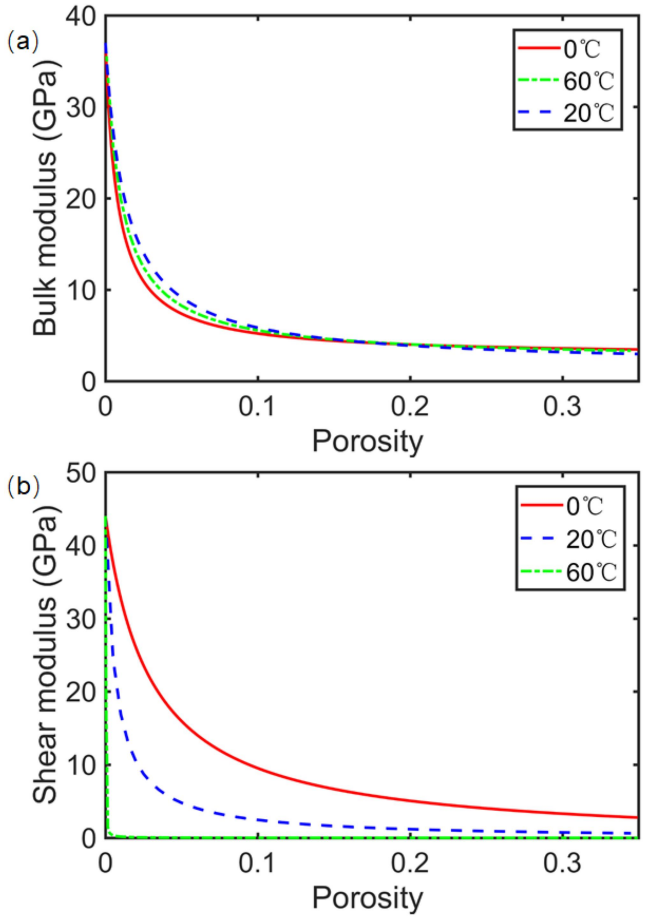

Figure 6. Bulk (a) and shear (b) moduli of Model II as a function of porosity.

Figure 2 shows the rock-physics modeling workflow.

3. Example

We consider pure-quartz oil sand with $K_s = 37$ GPa, $G_s = 44$ GPa, grain density $\rho_s = 2660$ kg/m^3, a porosity of 35%, the pore infill is heavy oil (API = 6.6°) according to Li et al. [47], the viscosity decreases with temperature and the fluid (liquid) point is 48.7 °C. Figure 3 shows the shear modulus of heavy oil with the viscoelastic Maxwell model. The infinite shear modulus (G_∞) decreases linearly with temperature and can be obtained by a linear regression fitting of the ultrasonic shear modulus [47]. As temperature increases and exceeds the liquid point, heavy oil becomes a fluid. At ultrasonic frequencies, its shear modulus approaches zero at approximately 48.7 °C and the viscosity is 1000 cP [25, 47].

3.1. Model I

Figure 4 shows the bulk and shear moduli as a function of porosity at different temperatures and at the ultrasonic frequency range. The moduli decrease with increasing porosity and slightly with increasing temperature.

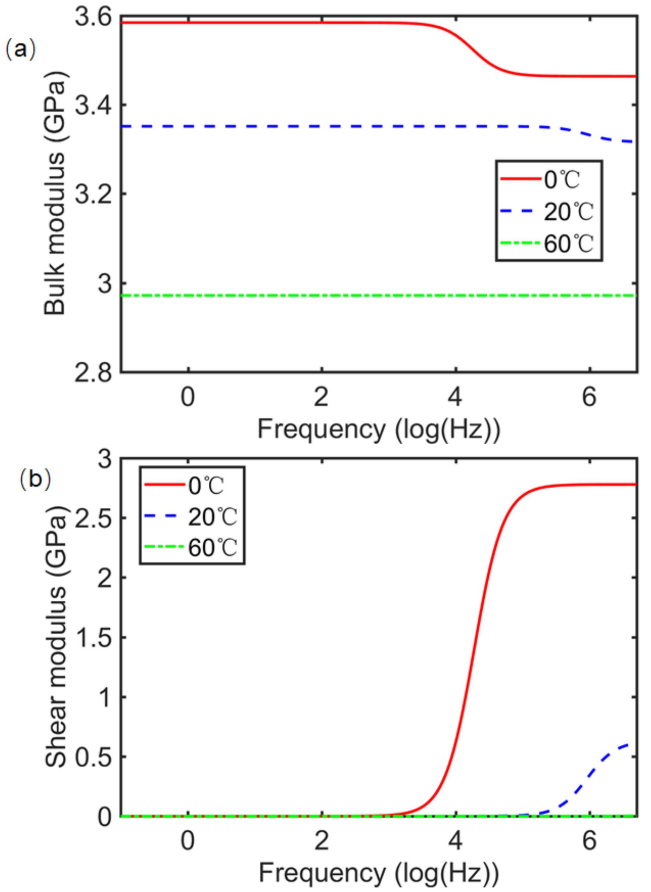

Figure 7. Bulk (a) and shear (b) moduli of Model II as a function of frequency.

The behavior as a function of frequency at different temperatures is shown in Figure 5, where we observe the lack of dispersion at high temperatures (fluid phase) and that the effects are noticeable at high frequencies.

3.2. Model II

Figures 6 and 7 show the moduli as a function of porosity and frequency, respectively for different temperatures, where we can see that the shear modulus is more affected and it is almost zero at high temperatures (fluid phase). As above, the dispersion effects are important at high frequencies.

3.3. Model III

In this case, heavy oil cements the grains. The contact thickness is assumed to be 0.001. Figures 8 and 9 show the moduli as a function of porosity and frequency, respectively for different temperatures. The behavior of these curves is qualitatively similar to those of the other two models, with no dispersion at high temperatures.

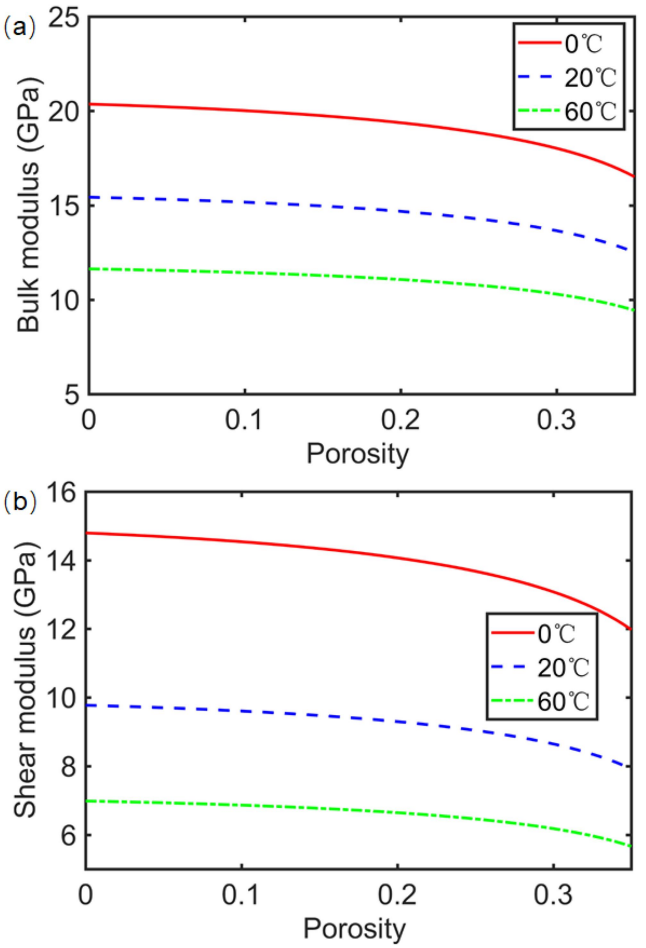

Figure 8. Bulk (a) and shear (b) moduli of Model III as a function of porosity.

Figure 10 shows the bulk and shear moduli of Model III as a function of temperature and contact thicknesses. The moduli decrease when both quantities increase.

3.4. Wave velocities

We substitute the effective moduli into Eqs. (7) and (8) to obtain the corresponding P- and S-wave velocities for the three models for two temperatures (Figure 11). For all the three types, the wave velocities are influenced by temperature variation. When temperature increases from 0 to 40 °C, the P- and S-wave velocities of Model I decrease by 6.69% and 8.06%, those of Model II by 32.75% and 85.10%, and those of Model III decrease by 23.88% and 26.82%, respectively. When heavy oil is at a quasi-solid state, the S-wave velocity is more sensitive to temperature, due to the contribution of the shear modulus. Furthermore, if heavy oil is the matrix, the wave responses are dominated by the oil, followed by the case of cement, where we assume a stronger cementation, which may improve the stiffnesses of the rock and its mechanical stability.

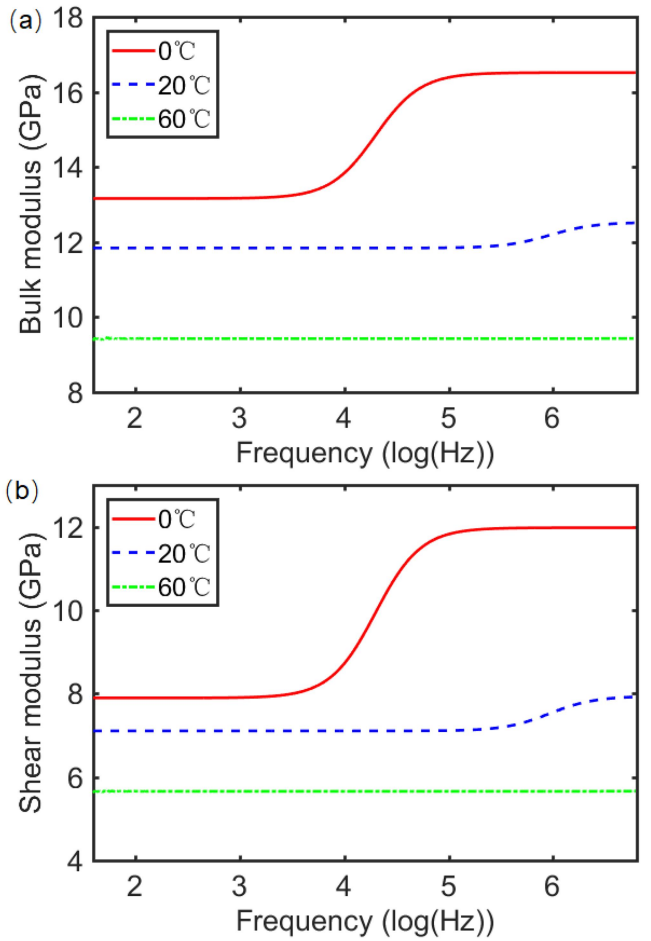

Figure 9. Bulk (a) and shear (b) moduli of Model III as a function of frequency.

4. Comparison with experimental data

4.1. Oil–sand samples

Experimental data of an oil–sand sample reported by Li et al. [47] and two oil sand samples reported by Yuan et al. [6] are considered in a comparative analysis with the model results. The main mineral components of sample 1 include quartz and clay, where pore infill is heavy oil with an API density of 6.6° and a liquid point of 48.7 °C. The frequency is 1 MHz and the pore pressure was set to 0 psi. The mineral of the other samples (2 and 3) is quartz, where the pore infill is heavy oil with an API density of 7.5°and a liquid point of 50 °C. The pore pressure is 334 psi. The specific properties of the samples are given in Table 1.

4.2. Estimating the distribution of heavy oil in sands

We consider the three models and the results are compared to the measured data.

4.2.1. Sample 1

Figure 12 shows the results for sample 1, where we can see that those of Model I are consistent with the experimental P- and S-wave velocities, indicating that this temperature-dependent model

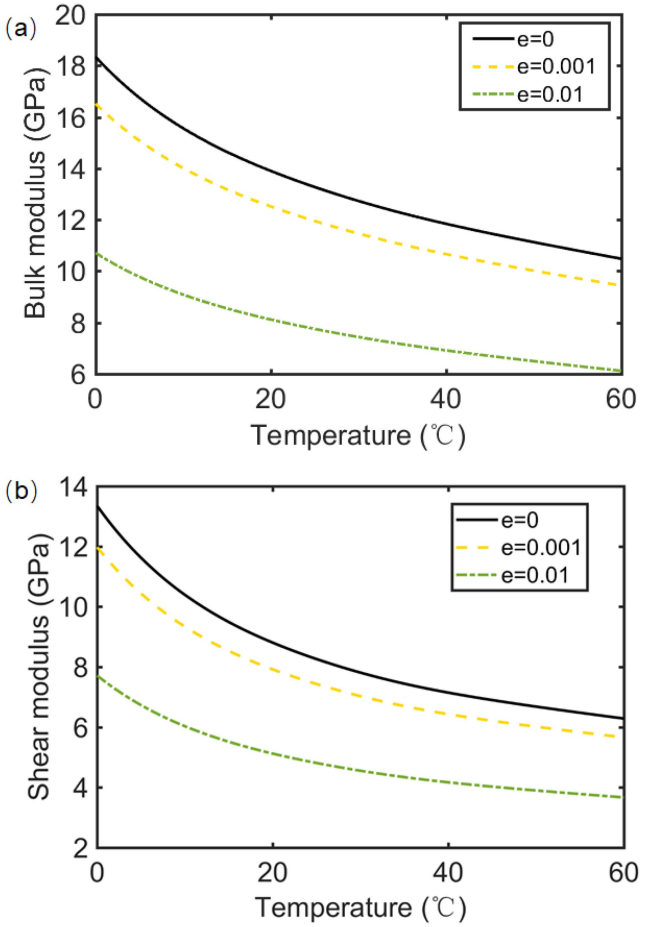

Figure 10. Bulk (a) and shear (b) moduli of Model III as a function of temperature and different contact thicknesses.

can quantitatively describe the wave response. The P-wave results of Model III are consistent with the data, but the S-wave is not. This model is based on heavy oil as cement, with $e = 0.001$. The normal and tangential contact stiffnesses are assumed constants in theory, but they may vary with temperature in actual experiments. Conversely, the results of Model II are the lowest ones. We conclude that Model I is the best.

4.2.2. Samples 2 and 3

Figure 13 shows the results for samples 2 and 3, where Model III better describes the data, i.e., there is cementation by the pore infill. The predicted results of Models I and II deviate from the experimental data. Figure 14 shows the velocity variation rates of samples 1 and 2 when the temperature increases from 12 °C to 60 °C. That of sample 1 is higher, because the viscosity of heavy

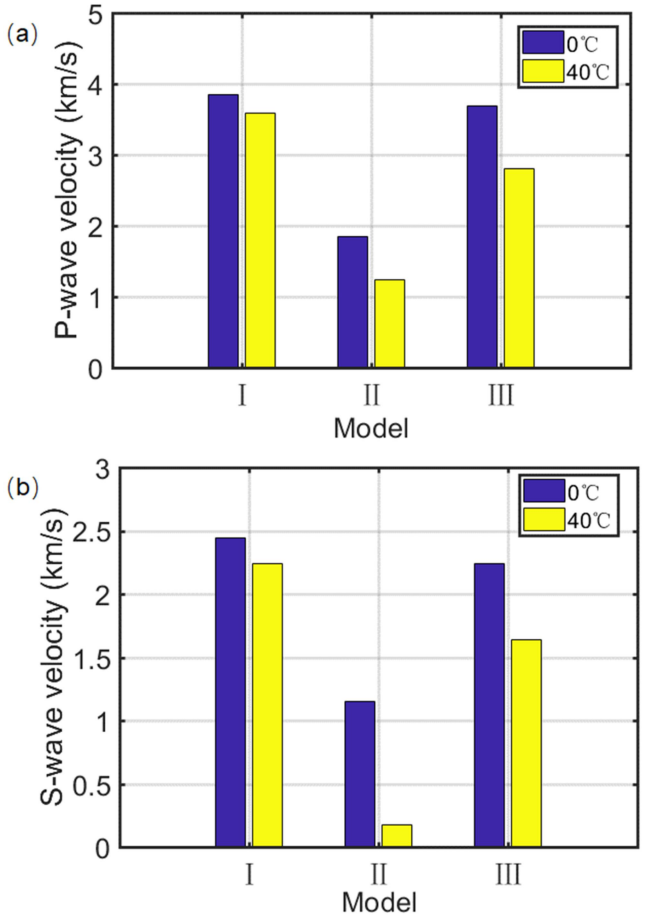

Figure 11. P-wave (a) and S-wave (b) velocities with respect to temperature for the three models.

Table 1. Physical properties of oil sands.

Rock type	Density (kg/m^3)	Porosity (%)	Grain density (kg/m^3)	Mineral bulk modulus (GPa)	Mineral shear modulus (GPa)
1	1970	42	2660	21.4	24.1
2	1980.88	41	2650	36	44
3	2029.84	38	2650	36	44

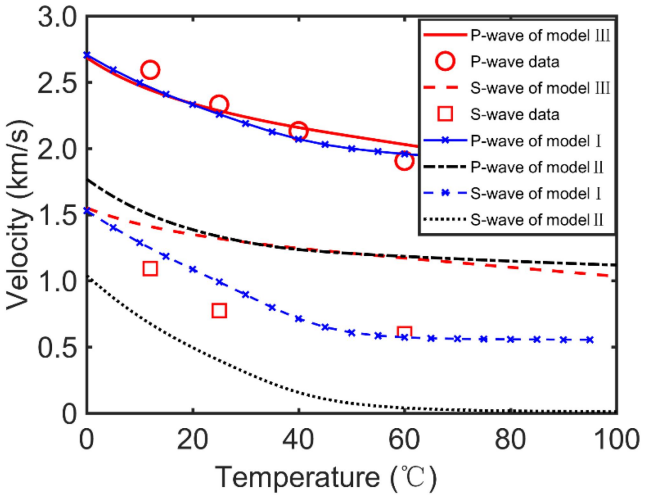

Figure 12. P- and S-wave velocities as a function of temperature for the three models compared to experimental data of sample 1.

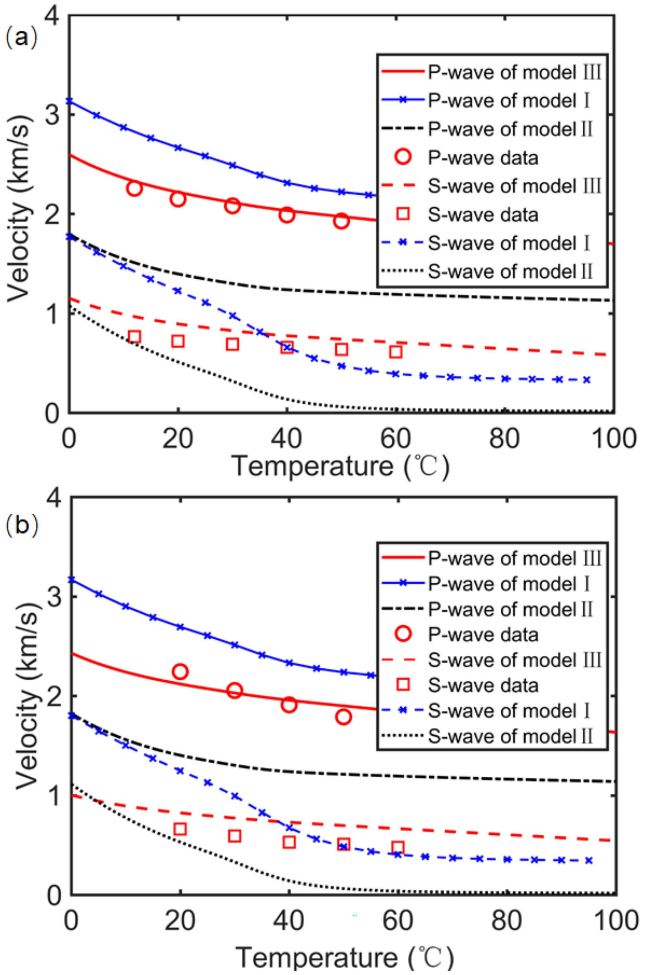

Figure 13. P- and S-wave velocities as a function of temperature for the three models and samples 2 (a) and 3 (b).

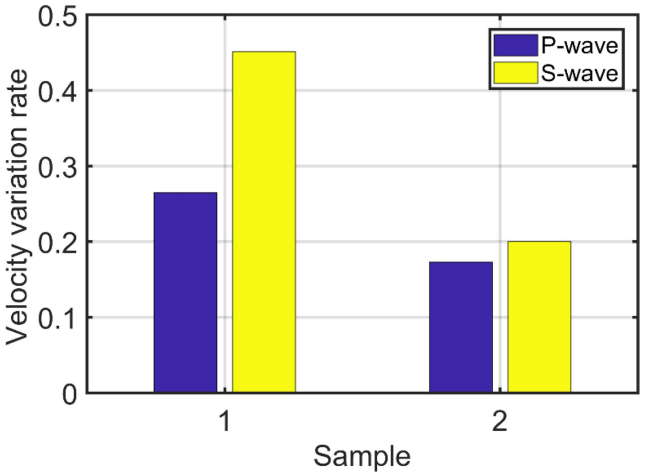

Figure 14. Velocity variation rate of samples 1 and 2 when the temperature increases from 12 °C to 60 °C.

oil in sample 1 is higher. The heavy oil in sample 1 is affected by temperature as a pore infill, while in sample 2 as a cement.

5. Conclusions

We analyze the temperature dependence of the P- and S-wave velocities (and moduli) of oil sand based on the different distribution and state of heavy oil. If heavy oil is a pore infill, the theory is based on the CPA (coherent potential approximation), double-porosity, Maxwell, and David–Zimmerman models. If the heavy oil is a continuous matrix, we use the Maxwell and HS^- (Hashin–Shtrikmann lower bound) equations. A third model considers oil as cement, and the wave response is described by a temperature-dependent CC (contact cement) theory combined with the Maxwell model. The results show that no matter how the heavy oil is distributed in the sand, the S-wave velocity is more sensitive to temperature variations. For all the models, the velocities decrease with porosity and temperature and the velocity dispersion is important at high frequencies and negligible at high temperatures. A comparison with experimental data may be used to estimate the heavy oil distribution, as pore infill, as skeleton (matrix) or as cement. It is showed that when the medium contains different distributions of heavy oil, the wave responses show different sensitivities to temperature. The three models may be used to infer characteristics about the microstructure of the oil sand.

Disclosure statement

The authors declare that they have no known competing financial interests or personal relationships that could have appeared to influence the work reported in this article.

Funding

This work is supported by the National Natural Science Foundation of China (grant no. 41974123 and 42174161), the Jiangsu Province Science Fund for Distinguished Young Scholars (grant no. BK20200021) and research fund of North China University of Water Resources and Electric Power (No. 202209020).

References

[1] J. Behura, M. Batzle, R. Hofmann, and J. Dorgan, "Heavy oils - their shear story," *Geophysics*, vol. 72, no. 5, pp. E175–E183, 2007. DOI: 10.1190/1.2756600.

[2] J. Eastwood, "Temperature-dependent propagation of P-waves and S-waves in Cold Lake oil sands: comparison of theory and experiment," *Geophysics*, vol. 58, no. 6, pp. 863–872, 1993. DOI: 10.1190/1.1443470.

[3] A. Nur, C. Tosaya, and D. V. Thanh, "Seismic monitoring of thermal enhanced oil recovery processes," presented at the 54th Annual International Meeting, SEG, Expanded Abstracts, Atlanta, Georgia, USA, 1984, pp. 337–340. DOI: 10.1190/1.1894015.

[4] D. R. Schmitt, "Seismic attributes for monitoring of a shallow heated heavy oil reservoir: a case study," *Geophysics*, vol. 64, no. 2, pp. 368–377, 1999. DOI: 10.1190/1.1444541.

[5] J. W. Spencer, "Viscoelasticity of Ells River bitumen sand and 4D monitoring of thermal enhanced oil recovery processes," *Geophysics*, vol. 78, no. 6, pp. D419–D428, 2013. DOI: 10.1190/geo2012-0535.1.

[6] H. Yuan, D. H. Han, H. Li, and W. Zhang, "A comparison of bitumen sands and bitumen carbonates: measured data," *Geophysics*, vol. 82, no. 1, pp. MR39–MR50, 2017. DOI: 10.1190/geo2015-0657.1.

[7] J. Guo and X. Han, "Rock physics modelling of acoustic velocities for heavy oil sand," *J. Pet. Sci. Eng.*, vol. 145, pp. 436–443, 2016. DOI: 10.1016/j.petrol.2016.05.028.

[8] B. Gurevich, K. Osypov, R. Ciz, and D. Makarynska, "Modeling elastic wave velocities and attenuation in rocks saturated with heavy oil," *Geophysics*, vol. 73, no. 4, pp. E115–E122, 2008. DOI: 10.1190/1.2940341.

[9] D. H. Han, Q. Yao, and H. Z. Zhao, "Complex properties of heavy oil sand," presented at the 77th Annual International Meeting, SEG, Expanded Abstracts, San Antonio, 2007, pp. 1609–1613.

[10] D. H. Han, H. Z. Zhao, and Q. Yao, "Velocity of heavy oil sand," presented at the 77thAnnual International Meeting, SEG, Expanded Abstracts, San Antonio, 2007, pp. 1619–1623.

[11] D. H. Han, J. Liu, and M. Batzle, "Seismic properties of heavy oils—measured data," *Lead. Edge*, vol. 27, no. 9, pp. 1108–1115, 2008. DOI: 10.1190/1.2978972.

[12] D. Makarynska, B. Gurevich, J. Behura, and M. Batzle, "Fluid substitution in rocks saturated with viscoelastic fluids," *Geophysics*, vol. 75, no. 2, pp. E115–E122, 2010. DOI: 10.1190/1.3360313.

[13] H. M. Yuan, D. H. Han, and W. Zhang, "Heavy oil sands modeling during thermal production and its seismic response," *Geophysics*, vol. 81, no. 1, pp. D57–D70, 2016. DOI: 10.1190/geo2014-0573.1.

[14] K. Wolf, T. Mukerji, and G. Mavko, "Attenuation and velocity dispersion modeling of bitumen saturated sand," presented at the 76th Annual International Meeting, SEG, Expanded Abstracts, New Orleans, LA, United States, 2006, pp. 1993–1997. DOI: 10.1190/1.2369925.

[15] J. C. Maxwell, "On the dynamical theory of gases," *Philos. Trans. Roy. Soc. Lond.*, vol. 157, pp. 49–88, 1867.

[16] R. Ciz and S. Shapiro, "Generalization of Gassmann equations for porous media saturated with a solid material," *Geophysics*, vol. 72, no. 6, pp. A75–A79, 2007. DOI: 10.1190/1.2772400.

[17] R. Brown and J. Korringa, "On the dependence of the elastic properties of a porous rock on the compressibility of the pore fluid," *Geophysics*, vol. 40, no. 4, pp. 608–616, 1975. DOI: 10.1190/1.1440551.

[18] F. Gassmann, "Über die ElastizitätporöserMedien," *Vierteljahrsschriftder NaturforschendenGesselschaft Zürich*, vol. 96, pp. 1–23, 1951.

[19] A. Kato and D. H. Han, "Volume viscosity and its induced bulk modulus of heavy oil," 71st European Association of Geoscientists and Engineers Conference and Exhibition 2009: Balancing Global Resources. Incorporating SPE EUROPEC, Amsterdam, Netherlands, 2009, vol. 6, pp. 3948–3952.

[20] A. Das and M. Batzle, "A combined effective medium approach for modeling the viscoelastic properties of heavy oil reservoirs," presented at the 79th Annual International Meeting, SEG, Expanded Abstracts, Houston, TX, United States, 2009, pp. 2110–2114. DOI: 10.1190/1.3255273.

[21] J. G. Berryman, "Long-wavelength propagation in composite elastic media—I. Spherical inclusions, II ellipsoidal inclusions," *J. Acoust. Soc. Am.*, vol. 68, no. 6, pp. 1809–1819, 1980. DOI: 10.1121/1.385171.

[22] B. E. Hornby, L. M. Schwartz, and J. A. Hudson, "Anisotropic effective medium modeling of the elastic properties of shales," *Geophysics*, vol. 59, no. 10, pp. 1570–1583, 1994. DOI: 10.1190/1.1443546.

[23] P. Sheng, "Effective medium theory of sedimentary rocks," *Phys. Rev. B Condens. Matter*, vol. 41, no. 7, pp. 4507–4512, 1990. DOI: 10.1103/physrevb.41.4507.

[24] P. Sheng, "Consistent modeling of the electrical and elastic properties of sedimentary rocks," *Geophysics*, vol. 56, no. 8, pp. 1236–1243, 1991. DOI: 10.1190/1.1443143.

[25] H. Qi, J. Ba, J. M. Carcione, and L. Zhang, "Temperature-dependent wave velocities of heavy-oil saturated rocks," *Lithosphere*, vol. 2021, no. 3, pp. 3018678, 2022. DOI: 10.2113/2022/3018678.

[26] K. C. Leurer and J. Dvorkin, "Viscoelasticity of precompacted unconsolidated sand with viscous cement," *Geophysics*, vol. 71, no. 2, pp. T31–T40, 2006. DOI: 10.1190/1.2187795.

[27] R. D. Mindlin, "Compliance of elastic bodies in contact," *J. Appl. Mech.*, vol. 16, no. 3, pp. 259–268, 1949. DOI: 10.1115/1.4009973.

[28] M. Batzle, B. Zadler, R. Hofmann, and D. H. Han, "Heavy oils—seismic properties," presented at the 74th Annual International Meeting, SEG, Expanded Abstracts, Denver, Colorado, 2004, pp. 1762–1765.
[29] M. Batzle, R. Hofmann, and D. H. Han, "Heavy oils—seismic properties," *Lead. Edge*, vol. 25, no. 6, pp. 750–756, 2006. DOI: 10.1190/1.2210074.
[30] J. Dvorkin, A. Nur, and H. Yin, "Effective properties of cemented granular materials," *Mech. Mater.*, vol. 18, no. 4, pp. 351–366, 1994. DOI: 10.1016/0167-6636(94)90044-2.
[31] Z. Hashin and S. Shtrikman, "A variational approach to the elastic behavior of multiphase materials," *J. Mech. Phys. Solids*, vol. 11, no. 2, pp. 127–140, 1963. DOI: 10.1016/0022-5096(63)90060-7.
[32] M. A. Biot, "Theory of propagation of elastic waves in a fluid saturated porous solid—II. Higher frequency range," *J. Acoust. Soc. Am.*, vol. 28, no. 2, pp. 179–191, 1956. DOI: 10.1121/1.1908241.
[33] C. Luo, J. Ba, and Q. Guo, "Probabilistic seismic petrophysical inversion with statistical double-porosity Biot-Rayleigh model," *GEOPHYSICS*, vol. 88, no. 3, pp. M157–M171, 2023. DOI: 10.1190/geo2022-0288.1.
[34] T. T. Wu, "The effect of inclusion shape on the elastic moduli of a two-phase material," *Int. J. Solids Struct.*, vol. 2, no. 1, pp. 1–8, 1966. DOI: 10.1016/0020-7683(66)90002-3.
[35] E. C. David and R. W. Zimmerman, "Pore structure model for elastic wave velocities in fluid-saturated sandstones," *J. Geophys. Res.*, vol. 117, no. B7, pp. B07210, 2012. DOI: 10.1029/2012JB009195.
[36] J. M. Carcione, B. Farina, F. Poletto, A. N. Qadrouh, and W. Cheng, "Seismic attenuation in partially molten rocks," *Phys. Earth Planet. Inter.*, vol. 309, no. 1, pp. 106568, 2020. DOI: 10.1016/j.pepi.2020.106568.
[37] R. Ciz, E. H. Saenger, B. Gurevich, and S. A. Shapiro, "Temperature-dependent poroelastic and viscoelastic effects on microscale - modelling of seismic reflections in heavy oil reservoirs," *Geophys. J. Roy. Astron. Soc.*, vol. 176, no. 3, pp. 822–832, 2009. DOI: 10.1111/j.1365-246X.2008.04016.x.
[38] R. Hill, "A self-consistent mechanics of composite materials," *J. Mech. Phys. Solids*, vol. 13, no. 4, pp. 213–222, 1965. DOI: 10.1016/0022-5096(65)90010-4.
[39] S. Picotti, J. M. Carcione, and J. Ba, "Rock-physics templates for seismic Q," *Geophysics*, vol. 84, no. 1, pp. MR13–MR23, 2019. DOI: 10.1190/geo2018-0017.1.
[40] A. Reuss, "Calculation of the flow limits of mixed crystals on the basis of the plasticity of monocrystals," *Z. Angew. Math. Mech.*, vol. 9, no. 1, pp. 49–58, 1929. DOI: 10.1002/zamm.19290090104.
[41] W. Voigt, Lehrbuch der Kirstallphysik: Teubner, 1910.
[42] R. W. Zimmerman and M. S. King, "The effect of the extent of freezing on seismic velocities in unconsolidated permafrost," *Geophysics*, vol. 51, no. 6, pp. 1285–1290, 1986. DOI: 10.1190/1.1442181.
[43] G. Mavko, T. Mukerji, and J. Dvorkin, *Rock Physics Handbook: Tools for Seismic Interpretation in Porous Media*. Cambridge, UK: Cambridge University Press, 1998.
[44] B. Gurevich, K. Osypov, and R. Ciz, "Viscoelastic modelling of rocks saturated with heavy oil," presented at the 77th Annu. Int. Meet.," SEG Expanded Abstracts, 2007, pp. 1614–1618.
[45] X. Han, J. Guo, F. Li, L. Yang, and J. Tang, "Modified acoustic velocity model for basal cemented loose sandstone based on contact cement theory," *J. China Univ. Pet.*, vol. 37, no. 4, pp. 76–82, 2013.
[46] X. Han, J. Guo, F. Li, and L. Yang, "Generalization of the expression of cementation radius in Contact Cement Theory and its application," *Chin. J. Geophys.*, vol. 57, no. 7, pp. 2235–2243, 2014.
[47] H. Li, L. Zhao, D. H. Han, M. Sun, and Y. Zhang, "Elastic properties of heavy oil sands: effects of temperature, pressure, and microstructure," *Geophysics*, vol. 81, no. 4, pp. D453–D464, 2016. DOI: 10.1190/geo2015-0351.1.